AIMS Materials Science, 6(2): 214–233.
DOI: 10.3934/matersci.2019.2.214
Received: 16 December 2018
Accepted: 13 March 2019
Published: 25 March 2019

http://www.aimspress.com/journal/Materials

Research article

Optimum reductants ratio for CO_2 reduction by overlapped Cu/TiO_2

Akira Nishimura[1,*], Ryuki Toyoda[1], Daichi Tatematsu[1], Masafumi Hirota[1], Akira Koshio[2], Fumio Kokai[2] and Eric Hu[3]

[1] Division of Mechanical Engineering, Graduate School of Engineering, Mie University, Tsu, Mie, 514-8507, JAPAN
[2] Division of Chemistry for Materials, Graduate School of Engineering, Mie University, Tsu, Mie, 514-8507, JAPAN
[3] School of Mechanical Engineering, the University of Adelaide, Australia

*** Correspondence:** Email: nisimura@mach.mie-u.ac.jp; Tel: +81592319747; Fax: +81592319747.

Abstract: Cu-doped TiO_2 (Cu/TiO_2) film photocatalyst was prepared by combination of sol-gel and dip-coating process, and pulse arc plasma method. The effect of Cu/TiO_2 photocatalyst on CO_2 reduction performance with reductants of H_2O and H_2 was investigated. In addition, this study investigated overlapping two Cu/TiO_2 coated on netlike glass fiber discs in order to utilize the light effectively as well as increase the amount of photocatalyst used for CO_2 reduction. The characterization of prepared Cu/TiO_2 film coated on netlike glass fiber was analyzed by SEM, EPMA, TEM and EELS. Furthermore, the CO_2 reduction performance of Cu/TiO_2 film was tested under illumination of Xe lamp with or without ultraviolet (UV) light, respectively. As a result, the best CO_2 reduction performance has been achieved under the condition of $CO_2/H_2/H_2O$ = 1:0.5:0.5 with UV light illumination as well as without UV light illumination. Under the illumination condition with UV light, the highest concentration of CO for Cu/TiO_2 overlapped is 1.4 times as large as that for single Cu/TiO_2, while the highest concentration of CH_4 for Cu/TiO_2 overlapped is 1.7 times as that for single Cu/TiO_2. Under the illumination condition without UV light, the highest molar quality of CO per weight of photocatalyst for Cu/TiO_2 overlapped is 1.1 times as that for single Cu/TiO_2. The theoretical molar ratio of CO_2/H_2O or CO_2/H_2 to produce CO is 1:1, while the theoretical molar ratio of CO_2/H_2O or CO_2/H_2 to produce CH_4 is 1:4. Since the molar ratio of $CO_2/H_2/H_2O$ = 1:0.5:0.5 can be regarded as the molar ratio of CO_2/total reductants = 1:1, it is believed that the results of this study follow the reaction schemes of CO_2/H_2O and CO_2/H_2.

Keywords: Cu/TiO_2 photocatalyst; CO_2 reduction; overlapping effect; reductant; visible light response

1. Introduction

Due to mass consumption of fossil fuels, global warming and fossil fuels depletion have become serious global environmental problems in the world. After the industrial revolution, the averaged concentration of CO_2 in the world has been increased from 278 ppmV to 403 ppmV by 2016 [1]. Therefore, it is necessary to develop a new CO_2 reduction or utilization technology in order to recycle CO_2.

The application of CO_2 as a raw material in order to produce chemicals and energy compromises a way to diminish the CO_2 accumulation in the atmosphere [2]. If we consider energy producing possibilities, one possibility is the photochemical conversion of CO_2 into value-added chemicals which could be used as fuel [3].

The most widely used photocatalyst for the photocatalytic reactions is TiO_2 due to its availability, chemical stability, low cost and resistance to corrosion [4]. It is well known that CO_2 can be reduced into fuels, e.g., CO, CH_4, CH_3OH and H_2 etc. by using TiO_2 as the photocatalyst under ultraviolet (UV) light illumination [5–8]. However, pure TiO_2 has the limitation. It is only active when irradiated by UV light, which is not effective under sunlight. Since the solar spectrum only consists of about 4% of UV light, sunlight is not able to active the TiO_2 effectively for photocatalystic reaction. In addition, TiO_2 has a high electron/hole pair recombination rate compared to the rate of chemical interaction with the adsorbed species for redox reactions [9].

Recently, studies on CO_2 photochemical reduction by TiO_2 have been carried out from the viewpoint of performance promotion by extending absorption wavelength towards visible region. It was reported that a transition metals doping is useful technique for extending the absorbance of TiO_2 into the visible region [10–14]. Noble metal doping such as Pt, Pd, Au and Ag [11], Au, Pd-three dimensionally ordered macroporous TiO_2 [12], composition materials formed by GaP and TiO_2 [13], nanocomposite CdS/TiO_2 combining two different band gap photocatalyst [14], carbon-based AgBr nanocomposited TiO_2 [15], have been attempted to overcome the shortcomings of the pure TiO_2. They could improve the CO_2 reduction performance, however, the concentrations in the products achieved in all the attempts so far were still low, ranging from 1 to 150 μmol/g-cat [11–15].

Though various metals have been used for doping [10–15], Cu is considered as a favorite candidate. Cu can extend the absorption band to 600–800 nm [16,17], which covers the whole visible light range. Cu-decorated TiO_2 nanorod thin film performed ten times yields as large as TiO_2 for C_2H_5OH production [18]. Cu loaded N/TiO_2 also showed the good performance which yielded eight times as large as TiO_2 for CH_4 production [19]. Even under UV light illumination condition, Cu-decorated TiO_2 nanorod film yielded ten times as large as TiO_2 for CH_4 production [20]. Noble metals such as Pt and Au are too expensive to be used in industrial scale. Therefore, Cu is the best candidate because of its high efficiency and low cost compared to noble metals. Due to its availability as well as above described characteristics, Cu is selected as the dopant in this study.

Since a reductant is necessary for CO_2 reduction to produce fuel, H_2O and H_2 are usually used as reductants according to the review papers [6,8]. To promote the CO_2 reduction performance of photocatalyst, it is important to select the optimum reductant which provides the proton (H^+) for the

reduction reaction. The reaction scheme of CO_2 reduction with H_2O is as follows [21–23]:
<Photocatalytic reaction>

$$TiO_2 + h\nu \rightarrow h^+ + e^- \quad (1)$$

<Oxidization>

$$H_2O + h^+ \rightarrow \bullet OH + H^+ \quad (2)$$

$$\bullet OH + H_2O + h^+ \rightarrow O_2 + 3H^+ \quad (3)$$

<Reduction>

$$CO_2 + 2H^+ + 2e^- \rightarrow CO + H_2O \quad (4)$$

$$CO + 8H^+ + 8e^- \rightarrow CH_4 \quad (5)$$

The reaction scheme of CO_2 reduction with H_2 is as follows [24]:
<Photocatalytic reaction>

$$TiO_2 + h\nu \rightarrow h^+ + e^- \quad (6)$$

<Oxidization>

$$H_2 + 2h^+ \rightarrow 2H^+ + 2e^- \quad (7)$$

<Reduction>

$$CO_2 + e^- \rightarrow \bullet CO_2^- \quad (8)$$

$$\bullet CO_2^- + H^+ + e^- \rightarrow HCOO^- \quad (9)$$

$$HCOO– + H^+ \rightarrow CO + H_2O \quad (10)$$

$$H^+ + e^- \rightarrow \bullet H \quad (11)$$

$$CO_2 + 8e^- + 8\bullet H \rightarrow CH_4 + 2H_2O \quad (12)$$

There are some reports on CO_2 reduction with either H_2O or H_2 [6,8]. However, the effect of using H_2O and H_2 together as reductants is not investigated well. Though a few studies using pure TiO_2 under $CO_2/H_2/H_2O$ condition were reported [24–26], the effect of ratio of CO_2, H_2 and H_2O as well as the effect of Cu doping with TiO_2 on CO_2 reduction performance of photocatalyst was not investigated previously.

In this paper, TiO_2 film is coated by combination of sol-gel and dip-coating process on netlike glass fiber (SILIGLASS U, Nihonmuki Co.). After the netlike glass fiber is dipped into TiO_2 sol solution, it is dried out and fired in the electric furnace. The netlike glass fiber is a net composed of glass fiber whose diameter is about 10 μm. The fine glass fibers are knitted, resulting that the diameter of aggregate fiber is about 1 mm. According to manufacture specifications of netlike glass fiber, the porous diameter of glass fiber is about 1 nm and the specific surface area is about 400 m^2/g. The netlike glass fiber consists of SiO_2 whose purity is over 96 wt%. The aperture of net is about 2 mm × 2 mm. Since the netlike glass fiber has a porous characteristics, it is believed that TiO_2 film is captured by netlike glass fiber easily during dipping into TiO_2 sol solution. In addition, it can be expected that a CO_2 absorption performance of prepared photocatalyst is promoted due to the porous

structure of netlike glass fiber.

Then, Cu is loaded on the TiO_2 coated netlike glass fiber by pulse arc plasma method which can emit nanosized Cu particles by applying high electrical potential difference. The amount of loaded Cu can be controlled by the pulse number. In the present study, the pulse number is set at 100.

In the present paper, Cu/TiO_2 prepared was characterized by Scanning Electron Microscope (SEM) and Electron Probe Micro Analyzer (EPMA), Transmission Electron Microscope (TEM), Energy Dispersive X-ray Spectrometry (EDX) and Electron Energy Loss Spectrum (EELS) analysis. The CO_2 reduction performance with H_2 and H_2O under the condition of illuminating Xe lamp with or without UV light was investigated. The molar ratio of $CO_2/H_2/H_2O$ was changed for 1:1:1, 1:0.5:1, 1:1:0.5, 1:0.5:0.5 to clarify the optimum combination of $CO_2/H_2/H_2O$ for CO_2 reduction with Cu/TiO_2. In addition, the effect of overlapping two layers of Cu/TiO_2 coated netlike glass fiber on CO_2 reduction performance was investigated.

2. Experiment

2.1. Preparation of Cu/TiO_2 film

The combination of sol-gel and dip-coating process was used for preparing TiO_2 film. TiO_2 sol solution was made by mixing $[(CH_3)_2CHO]_4Ti$ (purity of 95 wt%, Nacalai Tesque Co.) of 0.3 mol, anhydrous C_2H_5OH (purity of 99.5 wt%, Nacalai Tesque Co.) of 2.4 mol, distilled water of 0.3 mol, and HCl (purity of 35 wt%, Nacalai Tesque Co.) of 0.07 mol. Netlike glass fiber was cut to disc, and its diameter and thickness were 50 mm and 1 mm, respectively. The netlike glass fiber disc was dipped into TiO_2 sol solution at the speed of 1.5 mm/s and pulled up at the fixed speed of 0.22 mm/s. Then, it was dried out and fired under the controlled firing temperature (*FT*) and firing duration time (*FD*), resulting that TiO_2 film was fastened on the netlike glass fiber. *FT* and *FD* were set at 623 K and 180 s, respectively. Cu was loaded on TiO_2 film by pulse arc plasma method. The pulse arc plasma gun device (ULVAC, Inc., ARL-300) having Cu electrode whose diameter was 10 mm was applied for Cu loading. After the netlike glass fiber coated with TiO_2 was set in chamber of the pulse arc plasma gun device which was vacuumed, the nanosized Cu particles were emitted from Cu electrode with applying the electrical potential difference of 200 V. The pulse arc plasma gun can evaporate Cu particle over the target in the circle area whose diameter is 100 mm when the distance between Cu electrode and the target is 160 mm. Since the difference between Cu electrode and TiO_2 film was 150 nm in the present study, Cu particle can be evaporated over TiO_2 film uniformly. The amount of loaded Cu was controlled by the pulse number. In the present paper, the pulse number was set at 100. Since the netlike glass fiber is transparent, the light can pass through the netlike glass fiber. The present study has also investigated if two layers of two Cu/TiO_2 coated on netlike glass fiber put on the top of the other (with certain distance, i.e., overlapping), what impact/improvement would be on the CO_2 reduction performance. The overlapping two layers of Cu/TiO_2 coated netlike glass fiber is expected to utilize the light effectively as well as to increase the amount of photocatalyst used for CO_2 reduction.

2.2. Characterization of Cu/TiO_2 film

The structure and crystallization characteristics of Cu/TiO_2 film were evaluated by SEM

(JXS-8530F, JEOL Ltd.), EPMA (JXA-8530F, JEOL Ltd.), TEM (JEM-2100/HK, JEOL Ltd.), EDX (JEM-2100F/HK, JEOL Ltd.) and EELS (JEM-ARM2007 Cold, JEOL Ltd.). Since these measurement instruments use electron for analysis, the sample should be an electron conductor. Since netlike glass disc was not an electron conductor, the carbon vapor deposition was conducted by the dedicated device (JEE-420, JEOL Ltd.) for Cu/TiO_2 coated on netlike glass disc before analysis. The thickness of carbon deposited on sample was approximately 20–30 nm.

The electron probe emits the electrons to the sample under the acceleration voltage of 15 kV and the current of 3.0×10^{-8} A, when the surface structure of sample is analyzed by SEM. The characteristic X-ray is detected by EPMA at the same time, resulting that the concentration of chemical element is analyzed according to the relationship between the characteristic X-ray energy and the atomic number. The spatial resolution of SEM and EPMA is 10 μm. The EPMA analysis helps not only to understand the coating state of prepared photocatalyst but also to measure the amount of doped metal within TiO_2 film on the base material.

The electron probe emits the electron to the sample under the acceleration voltage of 200 kV, when the inner structure of sample is analyzed by TEM. The size, thickness and structure of loaded Cu were evaluated. The characteristics X-ray is detected by EDX at the same time, resulting that the concentration distribution of chemical element toward thickness direction of the sample is analyzed. In the present paper, the concentration distribution of Ti and Cu were analyzed.

EELS can be applied not only for detecting elements but also determination of oxidation states of some transition metals. The EELS characterization was performed by JEM-ARM200F equipped with GIF Quantum having 2048 ch. The dispersion of 0.5 eV/ch can be achieved for the full width at half maximum of the zero loss peak.

2.3. CO_2 reduction experiment

Figure 1 shows that experimental set-up of the reactor consisting of stainless pipe (100 mm (*H.*) × 50 mm (*I.D.*)), a netlike glass disc coated with Cu/TiO_2 film (50 mm (*D.*) × 1 mm (*t.*)) which is located on the teflon cylinder (50 mm (*H.*) × 50 mm (*D.*)), a quartz glass disc (84 mm (*D.*) × 10 mm (*t.*)), a sharp cut filter which cuts off the light of wavelength below 400 nm (SCF-49.5C-42L, SIGMA KOKI CO. LTD.), a 150 W Xe lamp (L2175, Hamamatsu Photonics K. K.), mass flow controller, CO_2 gas cylinder and H_2 gas cylinder [27].

The reactor volume available for CO is 1.25×10^{-4} m^3. The light of Xe lamp, through the sharp cut filter and the quartz glass disc that are at the top of the stainless pipe, illuminates the netlike glass disc coated with Cu/TiO_2 film, which is located inside the stainless pipe. The wavelength of light from Xe lamp is ranged from 185 nm to 2000 nm. The Xe lamp can be fitted with a sharp cut filter to remove UV components of the light. With the filter, the wavelength from Xe lamp is ranged from 401 nm to 2000 nm. Figure 2 shows the light transmittance data of the sharp cut filter to prove the removal of the light whose wavelength is below 400 nm [27]. The average light intensity of Xe lamp on the photocatalyst without and with setting the sharp cut filter is 79.3 mW/cm^2 and 67.4 mW/cm^2, respectively.

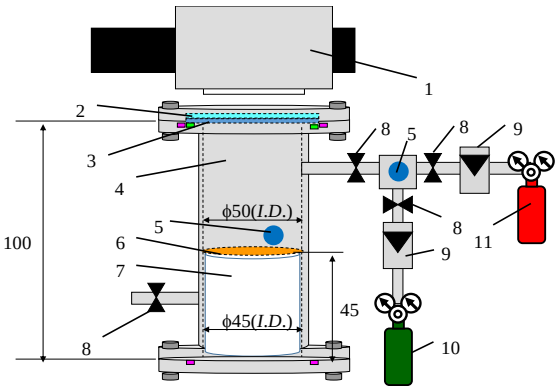

1. Xe lamp, 2. Sharp cut filter, 3. Quartz glass disc, 4. Stainless pipe,
5. Gas sampling tap, 6. Photocatalyst, 7. Teflon cylinder, 8. Valve,
9. Mass flow controller, 10. CO_2 gas cylinder (99.995 vol%),
11. H_2 gas cylinder (99.99999 vol%)

Figure 1. Schematic drawing of CO_2 reduction experimental set-up (Reprinted with permission from Ref. [27]).

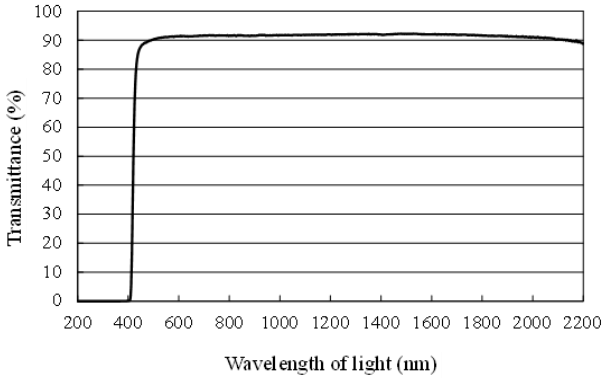

Figure 2. Light transmittance data of sharp cut filter (Reprinted with permission from Ref. [27]).

In the CO_2 reduction experiment, CO_2 gas with the purity of 99.995 vol% and H_2 gas with the purity of 99.9999 vol% which were controlled by mass flow controller were mixed in the buffer chamber, and introduced into the reactor which was pre-vacuumed by a vacuum pump. The mixing ratio of CO_2 and H_2 was confirmed by TCD gas chromatograph (Micro GC CP4900, GL Science) before introducing into the reactor. After confirming the mixing ratio of CO_2 and H_2, the distilled water was injected into the reactor through a gas sampling tap by syringe and Xe lamp illumination was turned on the same time. The amount of injected water was measured and controlled by the syringe. The injected water vaporized completely in the reactor. The molar ratio of $CO_2/H_2/H_2O$ was set at 1:1:1, 1:0.5:1, 1:1:0.5, 1:0.5:0.5. Due to the heat of Xe lamp, the temperature in reactor was attained at 343 K within an hour and kept at approximately 343 K during the experiment.

The gas in the reactor was sampled every 24 hour during the experiment. The gas samples were analyzed by FID gas chromatograph (GC353B, GL Science) and methanizer (MT221, GL Science). Minimum resolution of FID gas chromatograph and methanizer is 1 ppmV.

3. Results and discussion

3.1. Characterization of Cu/TiO_2 film

Figure 3 shows SEM image of Cu/TiO_2 film coated on netlike glass disc. The SEM image was taken at 1500 times magnification. Figure 4 shows EPMA images of Cu/TiO_2 film coated on netlike glass disc. EPMA analysis was carried out for SEM images taken by 1500 times magnification. In EPMA image, the concentrations of each element in observation area are indicated by the different colors. Light colors, for example, while, pink, and red indicate that the amount of element is large, while dark colors like black and blue indicate that the amount of element is small.

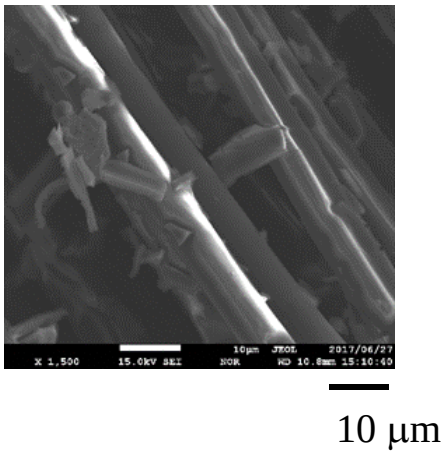

Figure 3. SEM image of Cu/TiO_2 film coated on netlike glass disc.

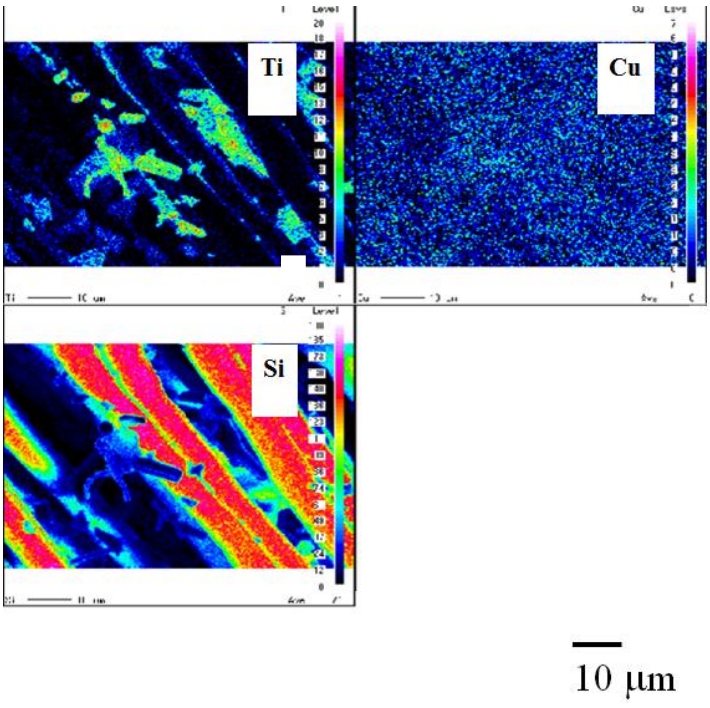

Figure 4. EPMA image of Cu/TiO_2 film coated on netlike glass disc.

From these figures, it can be observed that TiO_2 film was coated on netlike glass fiber. During firing process, the temperature profile of TiO_2 solution adhered on the netlike glass disc was not even due to the different thermal conductivities of Ti and SiO_2. Their thermal conductivities of Ti and SiO_2 at 600 K are 19.4 W/(m·K) and 1.82 W/(m·K), respectively [28]. Due to the thermal expansion and shrinkage around netlike glass fiber, it can be considered that thermal crack is formed on the TiO_2 film.

In addition, it is observed from Figure 4 that nanosized Cu particles are loaded on TiO_2 uniformly, resulted from that the pulse arc plasma method can emit nanosized Cu particles.

To evaluate the amount of loaded Cu within TiO_2 film quantitatively, the observation area, which is the center of netlike glass disc, of diameter of 300 μm is analyzed by EPMA. The ratio of Cu to Ti is counted by averaging the data obtained in this area. As a result, the weight percentages of elements of Cu and Ti in the Cu/TiO_2 film are 0.56 wt% and 99.44 wt%, respectively.

Figures 5 and 6 show TEM and EDX images of Cu/TiO_2 film, respectively. EDX analysis was carried out using TEM image taken by 150000 times magnification. According to Figure 6, it is observed that Cu particles are distributed in TiO_2 film. Though many Cu particles are loaded on the upside of TiO_2 film, it is not confirmed that the Cu layer is formed.

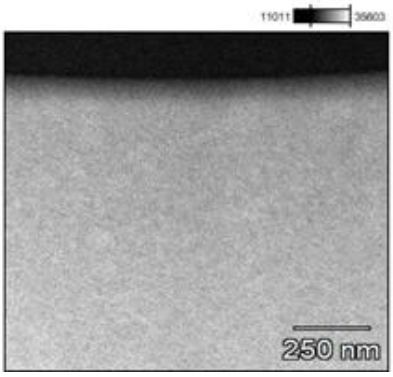

Figure 5. TEM image of Cu/TiO_2 film.

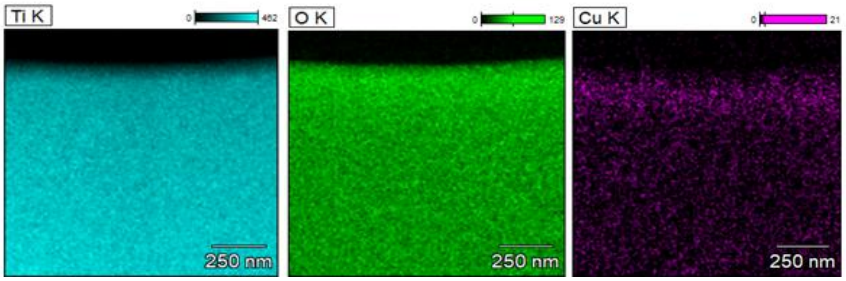

Figure 6. EDX images of Cu/TiO_2 film.

Figure 7 shows EELS spectra of Cu in Cu/TiO_2 film. From this figure, the peaks at around 932 eV and 952 eV can be observed. Compared to the report investigating the spectra peaks of Cu, Cu_2O and CuO [29], the EELS spectra of Cu_2O matches with Figure 7. Therefore, Cu in Cu/TiO_2

prepared in this study exists as Cu^{+} ion in Cu_2O. It was reported that the heterojunctions between CuO and TiO_2 contributed to the promotion of the photoactivity [30]. In addition, it was reported that Cu^{+} was more active than Cu^{2+} [31]. Therefore, it is expected that Cu^{+} would play a role to enhance the CO_2 reduction performance in this study. Figure 8 shows EELS spectra of TiO_2 referred from EELS data base [32]. Comparing Figure 8 with Figure 7, EELS spectra of TiO_2 is very different from EELS spectra of Cu in Cu/TiO_2.

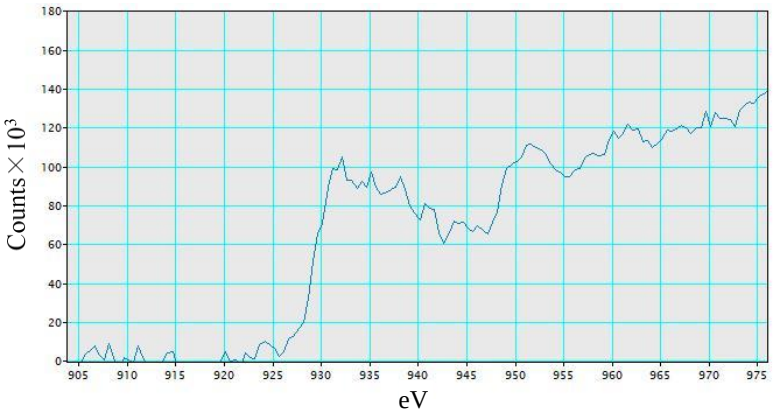

Figure 7. EELS spectra of Cu in Cu/TiO_2.

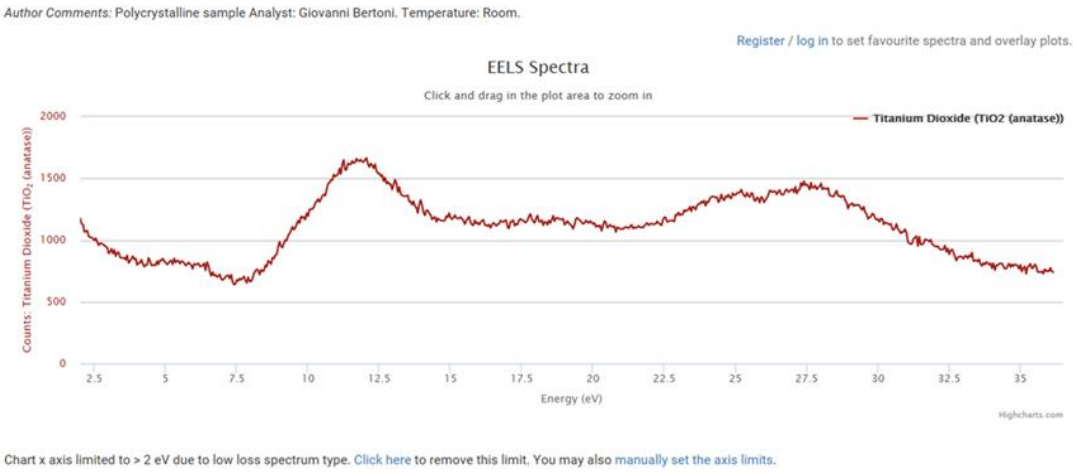

Figure 8. EELS spectra of TiO_2 referred from EELS data base [31].

3.2. Effect of molar ratio of CO_2, H_2 and H_2O on CO_2 reduction characteristics of Cu/TiO_2

Figures 9 and 10 show the concentration changes of CO and CH_4 produced in the reactor along the time under the illumination of Xe lamp with UV light on, respectively. Figures 11 and 12 show the molar quantities of CO and CH_4 per weight of photocatalyst in the reactor along the time under the illumination of Xe lamp with UV light on, respectively. The amount of Cu/TiO_2 is 0.16 g. In this experiment, a blank test, that was running the same experiment without illumination of Xe lamp, had been carried out to set up a reference case. No fuel was produced in the blank test as expected.

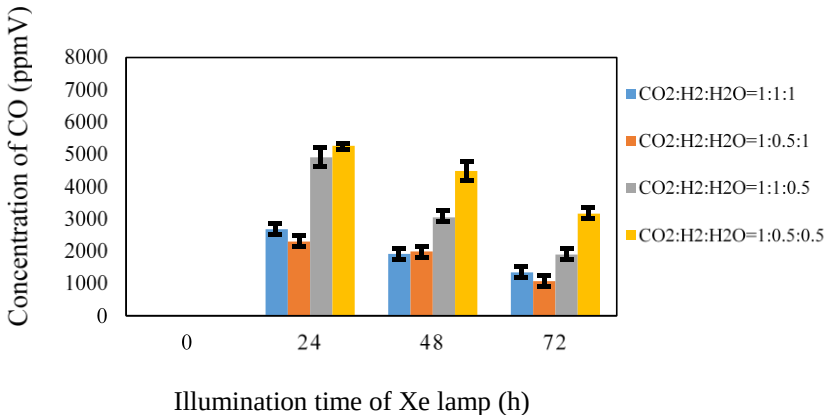

Figure 9. Change of concentration of CO with time for several molar ratios of $CO/H_2/H_2O$ under illumination condition with UV light.

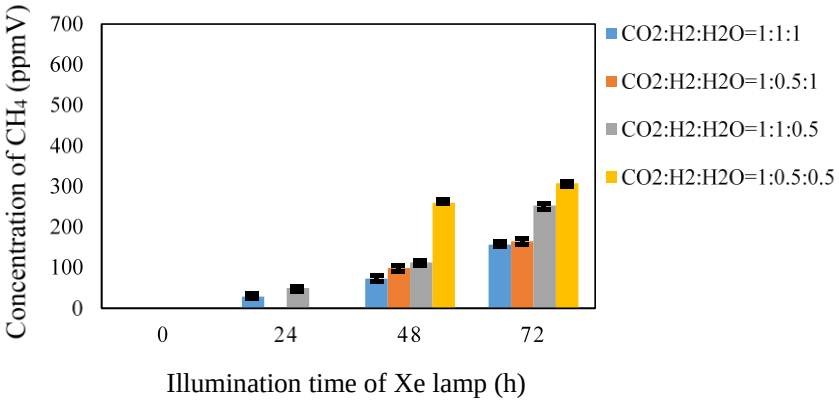

Figure 10. Change of concentration of CH_4 for several molar ratios of $CO/H_2/H_2O$ under illumination condition with UV light.

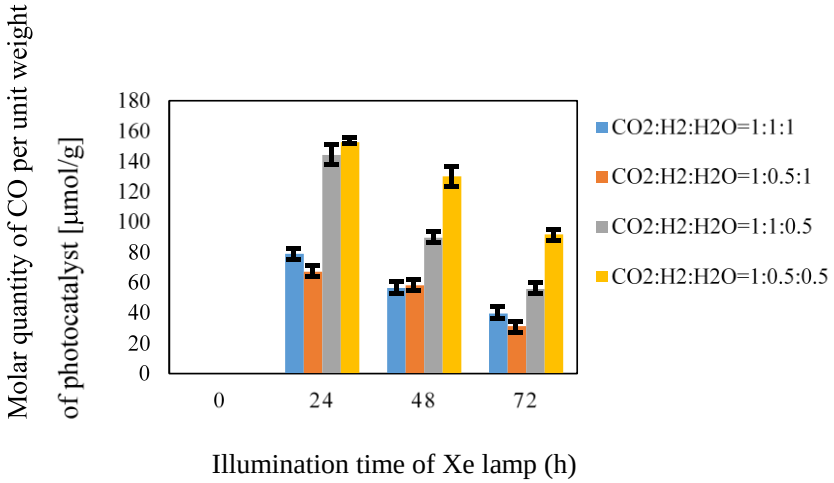

Figure 11. Change of molar quantity of CO per unit weight of photocatalyst with time for several molar ratios of $CO/H_2/H_2O$ under illumination condition with UV light.

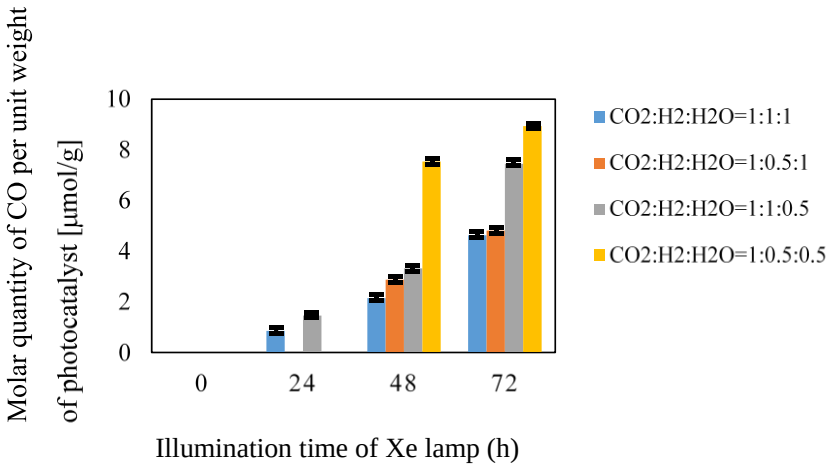

Figure 12. Change of molar quantity of CH_4 per unit weight of photocatalyst with time for several molar ratios of $CO/H_2/H_2O$ under illumination condition with UV light.

According to Figures 9, 10, 11 and 12, the CO_2 reduction performance is the highest for the molar ratio of $CO_2/H_2/H_2O$ = 1:0.5:0.5. Since the reaction scheme of $CO_2/H_2/H_2O$ is not fully understood, this study refers to the reaction scheme of CO/H_2O and CO_2/H_2 as shown by Eqs 1–12. It is known from the reaction scheme that the theoretical molar ratio of CO_2/H_2O and CO_2/H_2 to produce CO is 1:1. On the other hand, the theoretical molar ratio of CO_2/H_2O and CO_2/H_2 to produce CH_4 is 1:4. Since the molar ratio of $CO_2/H_2/H_2O$ = 1:0.5:0.5 can be regarded as the molar ratio of CO_2/total reductants = 1:1, it is believed that the results of this study follows reaction scheme presented in Eqs 1–12. Comparing the CO production with the CH_4 production, CO is produced first. According to Eq 5, it is believed that some CO might be converted into CH_4. Therefore, the start of CH_4 production is slower than that of CO production. Producing CH_4 needs four times H^+ and electrons as many as producing CO needs. Therefore, it is revealed that the optimum molar ratio of $CO/H_2/H_2O$ is decided by the CO production scheme. Though CO decreases after reaching the peak, CH_4 increases gradually.

According to Hinojosa-Reyes et al. [33], TiO_2 and Cu_2O formation leads to the photocatalytic activity since Cu_2O is a semiconductor with small band gap energy. In addition, Cu performs to avoid the electron and hole recombination and promote the charge transfer. In this study, it seems that the effect of Cu and Cu_2O on photoactivity is performed.

Figures 13 and 14 show the concentration changes of CO produced and the molar quantity of CO per weight of photocatalyst in the reactor under the illumination of Xe lamp without UV light on, respectively. In this experiment, CO is the only fuel produced from the reactions.

According to Figures 13 and 14, the CO_2 reduction performance is also the highest for the molar ratio of $CO_2/H_2/H_2O$ = 1:0.5:0.5 in this case. It is considered that the same reaction mechanism as mentioned above is conducted. The CO_2 reduction performance of Cu/TiO_2 under the illumination condition without UV light is lower than that under the illumination condition with UV light. Therefore, it can be claimed that Cu/TiO_2 obtains the main photoenergy from UV light.

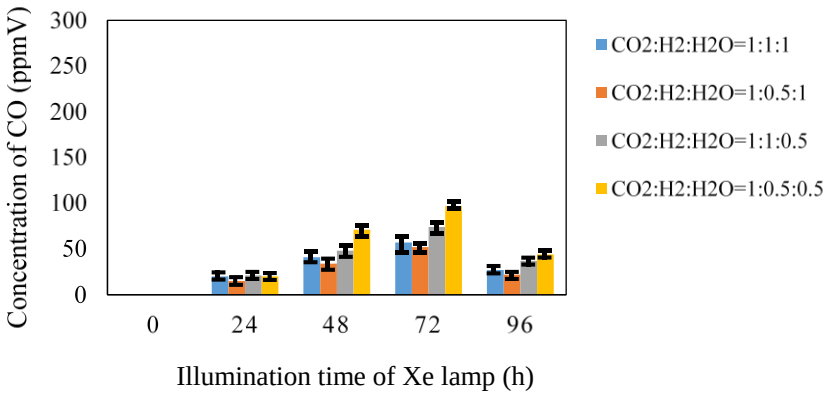

Figure 13. Change of concentration of CO with time for several molar ratios of $CO/H_2/H_2O$ under illumination condition without UV light.

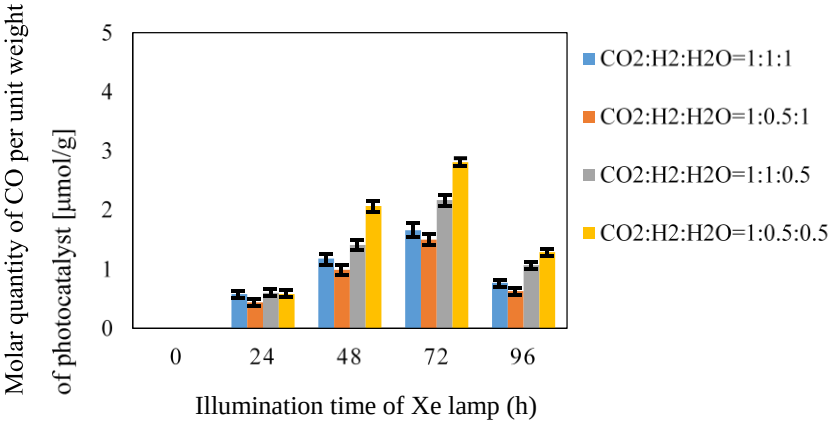

Figure 14. Change of molar quantity of CO per unit weight of photocatalyst with time for several molar ratios of $CO/H_2/H_2O$ under illumination condition without UV light.

3.3. Effect of overlapping on CO_2 reduction characteristics of Cu/TiO_2

Figures 15 and 16 show the concentration changes of CO and CH_4 produced in the reactor under the illumination of Xe lamp with UV light on, with two Cu/TiO_2 film coated on netlike glass discs overlapped, respectively. The photocatalyst is coated on both upper and lower surfaces of the top disc and only on the upper surface of the bottom disc.

Figures 17 and 18 show the molar quantities of CO and CH_4 per weight of photocatalyst in the reactor along the time under the Xe lamp with UV light on, respectively. The total amount of Cu/TiO_2 on two discs is 0.42 g.

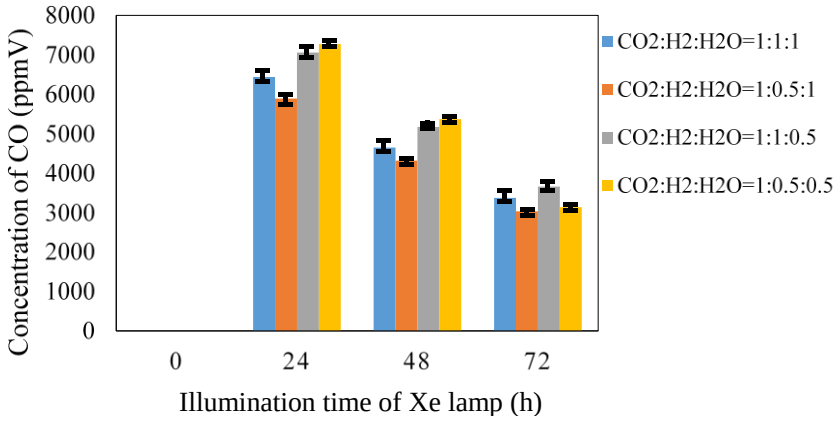

Figure 15. Change of concentration of CO for Cu/TiO_2 overlapped with time for several molar ratios of $CO/H_2/H_2O$ under illumination condition with UV light.

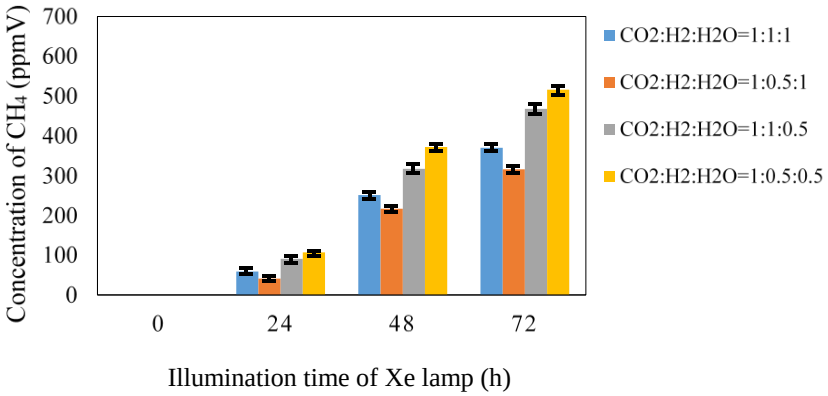

Figure 16. Change of concentration of CH_4 for Cu/TiO_2 overlapped with time for several molar ratios of $CO/H_2/H_2O$ under illumination condition with UV light.

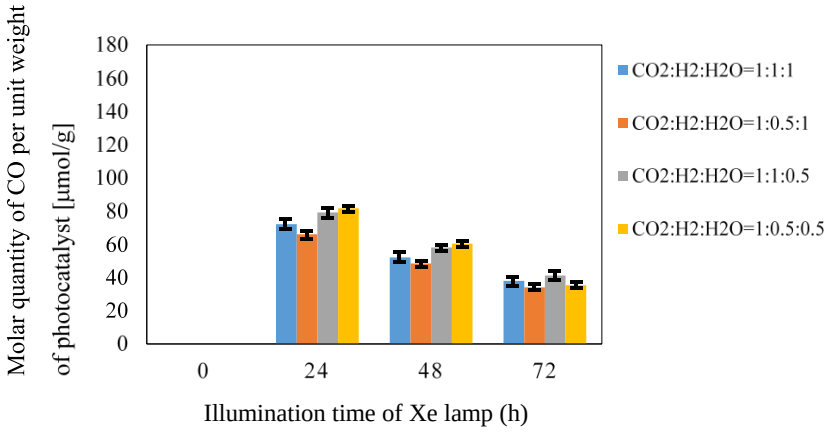

Figure 17. Change of molar quantity of CO per unit weight of photocatalyst for Cu/TiO_2 overlapped with time for several molar ratios of $CO/H_2/H_2O$ under illumination condition with UV light.

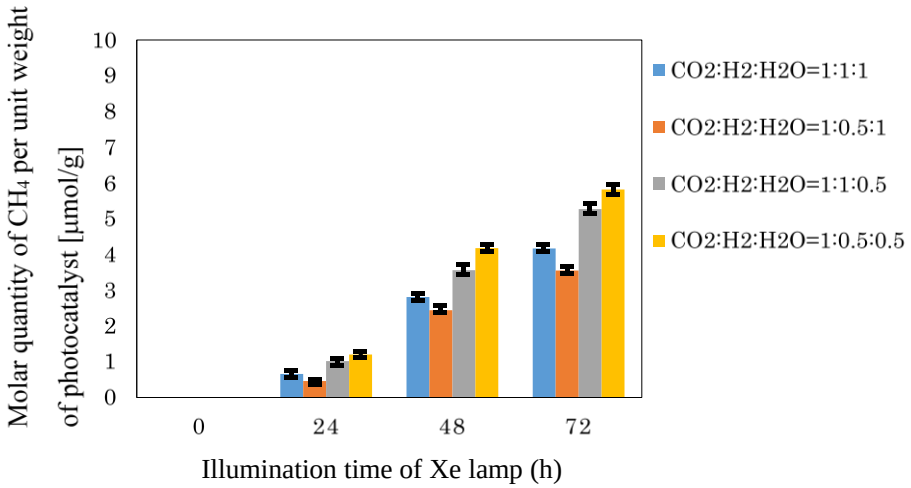

Figure 18. Change of molar quantity of CH_4 per unit weight of photocatalyst for Cu/TiO_2 overlapped with time for several molar ratios of $CO/H_2/H_2O$ under illumination condition with UV light.

According to Figures 15, 16, 17 and 18, the CO_2 reduction performance is the highest for the molar ratio of $CO_2/H_2/H_2O$ = 1:0.5:0.5, the same as that in the case of single Cu/TiO_2 disc. In addition, the order of CO_2 reduction performance of Cu/TiO_2 overlapped is the same as that of single Cu/TiO_2. However, comparing Figures 15 and 16 with Figures 9 and 10, the concentrations of CO and CH_4 for two Cu/TiO_2 discs overlapped are higher than those for single Cu/TiO_2 disc under every molar ratio of $CO_2/H_2/H_2O$. The highest concentration of CO for Cu/TiO_2 overlapped is 7273 ppmV, which is 1.4 times as large as that for single Cu/TiO_2. On the other hand, the highest concentration of CH_4 for Cu/TiO_2 overlapped is 516 ppmV, which is 1.7 times as large as that for single Cu/TiO_2. In the case of two discs overlapped, the following things are believed: (i) The amount of photocatalyst used for photocatalysis reaction is increased, (ii) The electron transfer between two Cu/TiO_2 films promotes the activity of photocatalysis reaction, (iii) The lower positioned Cu/TiO_2 disc utilizes the light passing through the top disc.

However, comparing Figures 17 and 18 with Figures 11 and 12, the molar quantities of CO and CH_4 per weight of photocatalyst in two discs case are lower than those for single Cu/TiO_2 disc case under every molar ratio of $CO_2/H_2/H_2O$. The highest molar quantity of CO per weight of photocatalyst in two discs overlapped case is 82 μmol/g, which is 54% of that in single disc case. Similarly, the highest molar quantity of CH_4 per weight of photocatalyst in two discs overlapped case is 5.8 μmol/g, which is 65% of that in single disc case. The reasons of this result are considered to be: (i) Some parts of the Cu/TiO_2 film on the lower positioned disc can't receive the light, (ii) If the produced fuel remains in the space between two discs, the reactants of CO_2, H_2 and H_2O would be blocked to reach the surface of photocatalyst, resulting that the photochemical reaction could not be carried out well even though the light is illuminated for photocatalyst.

Figures 19 and 20 show the concentration changes of CO produced and the molar quantity of CO per weight of photocatalyst in the reactor with two overlapped Cu/TiO_2 film coated on netlike glass disc under the illumination of Xe lamp without UV light on, respectively. In this experiment, CO is the only produced from the reactions.

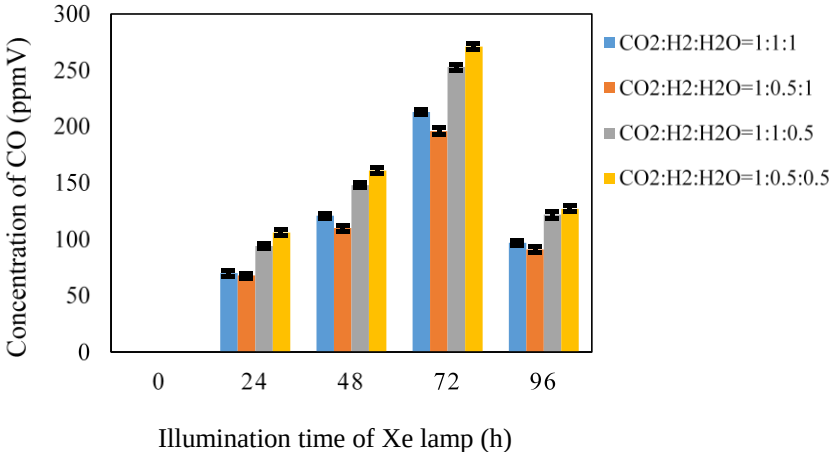

Figure 19. Change of concentration of CO for Cu/TiO_2 overlapped with time for several molar ratios of $CO/H_2/H_2O$ under illumination condition without UV light.

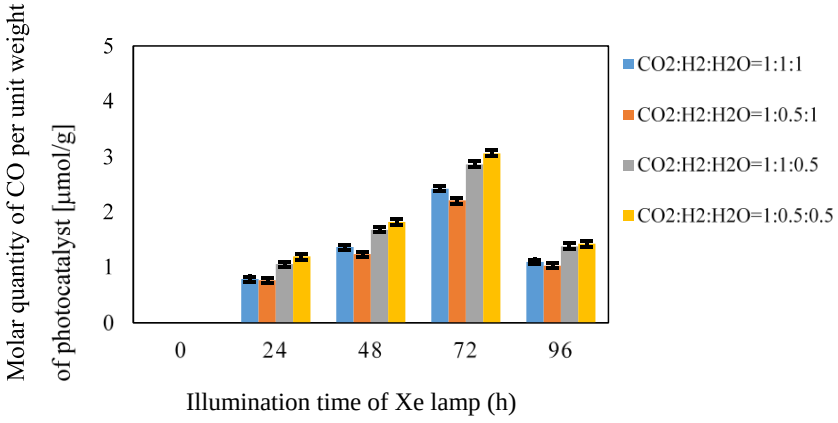

Figure 20. Change of molar quantity of CO per unit weight of photocatalyst for Cu/TiO_2 overlapped with time for several molar ratios of $CO/H_2/H_2O$ under illumination condition without UV light.

According to Figures 19 and 20, the CO_2 reduction performance in two discs case is the highest for the molar ratio of $CO_2/H_2/H_2O$ = 1:0.5:0.5 which is the same as that in the single disc case. The order of CO_2 reduction performance in two discs case is the same as that in the single disc case. However, comparing Figure 19 with Figure 13, the concentrations in two discs case are higher than those in single case under every molar ratio of $CO_2/H_2/H_2O$. The highest concentration of CO in two discs case is 271 ppmV, which is 2.8 times as large as that in single disc case. The same reasons explained in the case of illumination with UV light can be thought to cause the results.

In addition, comparing Figure 20 with Figure 14, the molar quantity of CO per weight of photocatalyst in two Cu/TiO_2 discs overlapped case is singly higher than that in the single disc case under every molar ratio of $CO_2/H_2/H_2O$. The highest molar quantity of CO per weight of photocatalyst is 3.1 μmol/g in two discs case, which is 1.1 times as large as that in the single disc case. Though the effect of overlapping layout is not obtained under the illumination condition with UV light, the effect of overlapping layout is confirmed under the illumination condition without UV

light. Since the photochemical reaction rate and the amount of produced fuel are small under the no-UV illumination condition compared to that with UV light, it would be beneficial to the mass transfer between produced fuels and reactants of CO_2, H_2 and H_2O on the surface of photocatalyst in no-UV cases [34]. As a result, the mass transfer and photochemical reaction are carried out effectively in no-UV cases. Therefore, the effect of overlapping layout is obtained in no-UV cases. According to the previous reports [35,36], the mass transfer is an inhibition factor to promote the CO_2 reduction performance of photocatalyst and it is necessary to control the mass transfer rate to meet the photochemical reaction rate. Figure 21 illustrates the comparison of mass and electron transfer within overlapped two photocatalysts in UV and no-UV illumination cases.

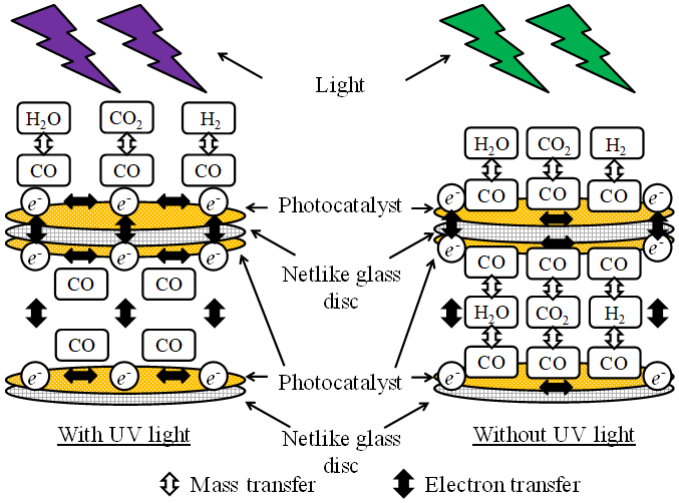

Figure 21. Comparison of mass and electron transfer within overlapped two photocatalysts between the illumination condition with UV light and without UV light.

In this study, the highest molar quantity of CO per weight of photocatalyst is 153 μmol/g in a single disc case under the illumination condition with UV light. The CO production performance achieved in this study is approximately 500 times as large as that reported in [24,26] which is owing to Cu doping. The CH_4 production performance achieved in this study is almost the same as that reported in [24]. Since the doped Cu provides the free electron preventing recombination of electron and hole produced as well as the improvement of the light absorption effect, the big improvement of CO_2 reduction performance is obtained in this study.

One way to further promote the CO_2 reduction performance may be that different metals should be doped on the higher and the lower positioned photocatalysts discs. The co-doped such as PbS-Cu/TiO_2, Cu-Fe/TiO_2, Cu-Ce/TiO_2, Cu-Mn/TiO_2 and Cu-CdS/TiO_2 would promote the CO_2 reduction performance of TiO_2 under the CO_2/H_2O condition [6,8]. When the combination of $CO_2/H_2/H_2O$ is considered, the ion number of dopant is important to match the number of electron emitted from the dopant with H^+ as shown by the reaction schemes of CO_2/H_2O and CO_2/H_2. The same number of electron and H^+ is necessary for fuel production. Though Cu^+ ion is applied to promote the CO_2 reduction performance with TiO_2 in this study, it is expected that the co-doping Cu and the other metal having larger positive ion might have positive effect for CO_2 reduction with H_2 and H_2O. In addition, the dopant like Fe, which can absorb the shorter wavelength light than

Cu [16,37,38], should be used at the higher positioned layer. The wavelength of light becomes long after penetrating the higher positioned photocatalyst [34]. Therefore, the overlapping of the higher positioned Fe/TiO_2 which absorbs the shorter wavelength light and the lower positioned Cu/TiO_2 which absorbs the longer wavelength light may be an effective way for utilization of wide range light. This idea is similar to the concept of hybridizing two photocatalysts having different band gaps [13,39,40].

4. Conclusion

Based on the investigation in this study, the following conclusions can be drawn:

(i) Cu in Cu/TiO_2 prepared by this study exists in the form of Cu^+ ion in Cu_2O.

(ii) The highest concentrations of CO and CH_4 produced as well as the highest molar quantities of CO and CH_4 per weight of photocatalyst for Cu/TiO_2 are obtained for $CO_2/H_2/H_2O$ ratio of 1:0.5:0.5. Since the molar ratio of $CO_2/H_2/H_2O$ = 1:0.5:0.5 can be regarded as the molar ratio of CO_2/total reductants = 1:1, it is believed that the results of this study follow reaction schemes of CO_2/H_2O and CO_2/H_2.

(iii) Under the illumination condition with UV light, the highest concentration of CO in two discs case is 1.4 times as large as that in the single disc case, while the highest concentration of CH_4 is 1.7 times. Under the illumination condition without UV light, the highest concentration of CO with two Cu/TiO_2 discs is 2.8 times as large as that with single Cu/TiO_2 disc.

(iv) Under the illumination condition with UV light, the highest molar quantity of CO per weight of photocatalyst with two Cu/TiO_2 discs overlapped is 54% of that with single Cu/TiO_2 disc. The highest molar quantity of CH_4 per weight of photocatalyst with two Cu/TiO_2 discs overlapped is 65% of that with single Cu/TiO_2 disc.

(v) Under the illumination condition without UV light, the molar quantity of CO per weight of photocatalyst with two Cu/TiO_2 discs overlapped is slightly (1.1 times) higher than that with single Cu/TiO_2 disc.

Acknowledgments

The authors would like to gratefully thank from JSPS KAKENHI Grant Number 16K06970, and joint research program of the Institute of Materials and Systems for Sustainability, Nagoya University for the financial support of this work.

Conflict of interest

The authors declare that there is no conflict of interest regarding the publication of this paper.

References

1. World Data Center for Greenhouse Gases. Available from: http://ds.data.jma.go.jp/gmd/wdcgg/wdcgg.html (accessed December 14, 2018).
2. Das S, Daud WMAW (2014) Photocatalytic CO_2 transformation into fuel: a review on advances in photocatalyst and photoreactor. *Renew Sust Energ Rev* 39: 765–805.

3. Tahir M, Amin NS (2013) Photocatalytic reduction of carbon dioxide with water vapors over montmorillonite modified TiO_2 nanocomposites. *Appl Catal B-Environ* 142–143: 512–522.
4. Tahir M, Amin NS (2015) Indium-doped TiO_2 nanoparticles for photocatalytic CO_2 reduction with H_2O vapors to CH_4. *Appl Catal B-Environ* 162: 98–109.
5. Abdullah H, Khan MMR, Ong HR, et al. (2017) Modified TiO_2 photocatalyst for CO_2 photocatalytic reduction: an overview. *J CO_2 Util* 22: 15–32.
6. Sohn Y, Huang W, Taghipour F (2017) Recent progress and perspectives in the photocatalytic CO_2 reduction of Ti-oxide-based nanomaterials. *Appl Surf Sci* 396: 1696–1711.
7. Neatu S, Macia-Agullo JA, Garcia H (2014) Solar light photocatalytic CO_2 reduction: general considerations and selected benchmark photocatalysts. *Int J Mol Sci* 15: 5246–5262.
8. Tahir M, Amin NS (2013) Advances in visible light responsive titanium oxide-based photocatalysts for CO_2 conversion to hydrocarbon fuels. *Energ Convers Manage* 76: 194–214.
9. Ola O, Maroto-Valer MM (2015) Review of material design and reactor engineering on TiO_2 photocatalysis for CO_2 reduction. *J Photoch Photobio C* 24: 16–42.
10. Wang JA, Limas-Ballesteros R, Lopez T, et al. (2001) Quantitative determination of titanium lattice defects and solid-state reaction mechanism in iron-doped TiO_2 photocatalysts. *J Phys Chem B* 105: 9692–9698.
11. Tan LL, Ong WJ, Chai SP, et al. (2015) Noble metal modified reduced graphene oxide/TiO_2 ternary nanostructures for efficient visible-light-driven photoreduction of carbon dioxide into methane. *Appl Catal B-Environ* 166–167: 251–259.
12. Jiao J, Wei Y, Zhao Y, et al. (2017) AuPd/3DOM-TiO_2 catalysts for photocatalytic reduction of CO_2: high efficient separation of photogenerated charge carries. *Appl Catal B-Environ* 209: 228–239.
13. Marci G, Garcia-Lopez EI, Palmisano L (2014) Photocatalytic CO_2 reduction in gas-solid regime in the presence of H_2O by using GaP/TiO_2 composite as photocatalyst under simulated solar light. *Catal Commun* 53: 38–41.
14. Beigi AA, Fatemi S, Salehi Z (2014) Synthesis of nanocomposite CdS/TiO_2 and investigation of its photocatalytic activity of CO_2 reduction to CO and CH_4 under visible light irradiation. *J CO_2 Util* 7: 23–29.
15. Fang Z, Li S, Gong Y, et al. (2014) Comparison of catalytic activity of carbon-based AgBr nanocomposites for conversion of CO_2 under visible light. *J Saudi Chem Soc* 18: 299–307.
16. Nagaveni K, Hegde MS, Madras G (2004) Structure and photocatalytic activity of $Ti_{1-x}M_xO_{2\pm\delta}$ (M = W, V, Ce, Zr, Fe, and Cu) synthesized by solution combustion method. *J Phys Chem B* 108: 20204–20212.
17. Yoong LS, Chong FK, Dutta BK (2009) Development of copper-doped TiO_2 photocatalyst for hydrogen production under visible light. *Energy* 34: 1652–1661.
18. Cheng M, Yang S, Chen R, et al. (2017) Copper-doped TiO_2 nanorod thin films in optofluidic planar reactors for efficient photocatalytic reduction of CO_2. *Int J Hydrogen Energ* 42: 9722–9732.
19. Khalid NR, Ahmed E, Niaz NA, et al. (2017) Highly visible light responsive metal loaded N/TiO_2 nanoparticles for photocatalytic conversion of CO_2 into methane. *Ceram Int* 43: 6771–6777.
20. Tan JZY, Fernández Y, Liu D, et al. (2012) Photoreduction of CO_2 using copper-decorated TiO_2 nanorod films with localized surface plasmon behavior. *Chem Phys Lett* 531: 149–154.

21. Goren Z, Willner I, Nelson AJ, et al. (1990) Selective photoreduction of CO_2/HCO_3^- to formate by aqueous suspensions and colloids of Pd-TiO_2. *J Phys Chem* 94: 3784–3790.
22. Tseng IH, Chang WC, Wu JCS (2002) Photoreduction of CO_2 using sol-gel derived titania and titania-supported copper catalysts. *Appl Catal B-Environ* 37: 37–38.
23. Nishimura A, Sugiura N, Fujita M, et al. (2007) Influence of preparation conditions of coated TiO_2 film on CO_2 reforming performance. *Kagaku Kogaku Ronbun* 33: 146–153.
24. Lo CC, Hung CH, Yuan CS, et al. (2007) Photoreduction of carbon dioxide with H_2 and H_2O over TiO_2 and ZrO_2 in a circulated photocatalytic reactor. *Sol Energ Mat Sol C* 91: 1765–1774.
25. Mahmodi G, Sharifnia S, Madani M, et al. (2013) Photoreduction of carbon dioxide in the presence of H_2, H_2O and CH_4 over TiO_2 and ZnO photocatalysts. *Sol Energy* 97: 186–194.
26. Jensen J, Mikkelsen M, Krebs FC (2011) Flexible substrates as basis for photocatalytic reduction of carbon dioxide. *Sol Energ Mat Sol C* 95: 2949–2958.
27. Nishimura A, Tatematsu D, Toyoda R, et al. (2019) Effect of Overlapping Layout of Fe/TiO_2 on CO_2 Reduction with H_2 and H_2O. *MOJ Solar Photoen Sys* 3: 1–8.
28. Japan Society of Mechanical Engineering (1993) *Heat Transfer Hand Book*, 1 Eds, Tokyo: Maruzen, 367–369.
29. Yang G, Cheng S, Li C, et al. (2014) Investigation of the oxidization states of Cu additive in colored borosilicate glasses by electron energy loss spectroscopy. *J Appl Phys* 116: 223707.
30. Qin S, Xin F, Liu Y, et al. (2011) Photocatalytic reduction of CO_2 in methanol to methyl formate over CuO-TiO_2 composite catalysts. *J Colloid Interf Sci* 356: 257–261.
31. Liu L, Gao F, Zhao H, et al. (2013) Tailoring Cu valence and oxygen vacancy in Cu/TiO_2 catalysts for enhanced CO_2 photoreduction efficiency. *Appl Catal B-Environ* 134–135: 349–358.
32. EELS data base. Available from: https://eelsdb.eu/spectra/titanium-dioxide-2/ (Accessed February 18, 2019).
33. Hinojosa-Reyes M, Camposeco-Solís R, Zanella R, et al. (2017) Hydrogen production by tailoring the brookite and Cu_2O ratio of sol-gel Cu-TiO_2 photocatalysts. *Chemosphere* 184: 992–1002.
34. Nishimura A, Zhao X, Hayakawa T, et al. (2016) Impact of overlapping Fe/TiO_2 prepared by sol-gel and dip-coating process on CO_2 reduction. *Int J Photoenergy* 2016: 2392581.
35. Nishimura A, Komatsu N, Mitsui G, et al. (2009) CO_2 reforming into fuel using TiO_2 photocatalyst and gas separation membrane. *Catal Today* 148: 341–349.
36. Nishimura A, Okano Y, Hirota M, et al. (2011) Effect of preparation condition of TiO_2 film and experimental condition on CO_2 reduction performance of TiO_2 photocatalyst membrane reactor. *Int J Photoenergy* 2011: 05650.
37. Ambrus Z, Balázs N, Alapi T, et al. (2008) Synthesis, structure and photocatalytic properties of Fe(III)-doped TiO_2 prepared from $TiCl_3$. *Appl Catal B-Environ* 81: 27–37.
38. Navío JA, Colón G, Litter MI, et al. (1996) Synthesis, characterization and photocatalytic properties of iron-doped titania semiconductors prepared from TiO_2 an iron(III) acetylacetonate. *J Mol Catal A-Chem* 106: 267–276.
39. Song G, Xin F, Chen J, et al. (2014) Photocatalytic reduction of CO_2 in cyclohexanol on CdS-TiO_2 heterostructured photocatalyst. *Appl Catal A-Gen* 473: 90–95.

40. Song G, Xin F, Yin X (2015) Photocatalytic reduction of carbon dioxide over $ZnFe_2O_4/TiO_2$ nanobelts heterostructure in cyclohexanol. *J Colloid Interf Sci* 442: 60–66.

AIMS Press